



Available online at www.sciencedirect.com



Nuclear Instruments and Methods in Physics Research B 212 (2003) 414–419

NIM B
Beam Interactions
with Materials & Atoms

www.elsevier.com/locate/nimb

Matrix and substrate effects on the sputtering of a 2 kDa molecule: Insights from molecular dynamics

A. Delcorde ^{a,*}, B. Arezki ^a, B.J. Garrison ^b

^a PCPM, Université catholique de Louvain, 1 Croix du Sud, 1348 Louvain-la-Neuve, Belgium

^b Department of Chemistry, The Pennsylvania State University, University Park, PA, USA

Abstract

In an effort towards a more accurate theoretical description of matrix and substrate effects in organic sputtering, we report on molecular dynamics simulations of the desorption induced by 500 eV Ar projectiles bombarding samples composed of polystyrene (PS) oligomers embedded in a trimethylbenzene matrix or cast on a silver substrate. The ejection of intact PS molecules, sometimes accompanied by matrix molecules/silver atoms, is observed in the first 10 ps following the impact. For the “matrix” sample, the results indicate that the emission of large amounts of organic material is mostly vibrationally induced. Extended calculations show that matrix:analyte clusters decay after emission, liberating the analyte in flight. In the case of the “substrate” sample, the emission is oftentimes the result of the concerted upward motion of several metal atoms underneath the molecule. Finally, the comparison between a matrix:analyte sample confined in a nanostructured silver crystal and a purely organic sample under identical bombardment conditions shows that the presence of the silver medium significantly enhances the desorption yields.

© 2003 Elsevier B.V. All rights reserved.

1. Introduction

The use of organic matrices [1–3] and metal substrates [4–6] constitute efficient methods to promote the desorption and ionization of large molecules in static secondary ion mass spectrometry. Even though a set of theoretical concepts and experimental evidences have been brought up over the years, a well established theory explaining the mode of action of the matrix/substrate in the emission process is still lacking. In particular, it is not clear what part of the matrix/substrate effect is due to specific ionization (electron, proton or

metal atom transfer) or desorption mechanisms (energy transfer, dissipation or reflection). The present study focuses on the desorption step of the molecular emission process, using molecular dynamics (MD) simulations to probe the different sputtering mechanisms at play when a polystyrene (PS) molecule is embedded in a low-molecular weight organic matrix or adsorbed on a heavy metal substrate.

2. Method

The Ar bombardment of *sec*-butyl terminated PS oligomers embedded in a trimethylbenzene (TMB) matrix or adsorbed on a silver monocrystal is modeled using MD computer simulations. The

* Corresponding author. Tel.: +32-10-473582; fax: +32-10-473452.

E-mail address: delcorde@pcpm.ucl.ac.be (A. Delcorde).

details of the simulation scheme are given elsewhere [7,8]. The energy and forces in the system are described by many-body interaction potentials. In particular, the C–C, C–H and H–H interactions are modeled by the AIREBO potential [9] including nonbonding interactions (van der Waals) through an adaptative treatment that conserves the reactivity of the reactive empirical bond-order potential [10,11]. For comparison purpose, three different samples have been synthesized in this study. The “substrate” (S) sample is simply constituted by a PS 16-mer deposited on top of a 9 layer silver microcrystallite, much like the samples described in [8]. The two other samples consist of PS 16-mers embedded in a TMB molecule matrix. These samples have been obtained via a step-by-step procedure alternating analyte/matrix molecule aggregation stages and sample relaxation stages in order to reach a minimum energy configuration. The “matrix” (M) sample is an aggregate of 4 PS 16-mers and 104 TMB molecules. Its shape is that of an ellipsoid with the revolution axis along the z -direction, i.e. the bombardment direction. The largest diameter of the ellipsoid is 50 Å and its equatorial diameter is 35 Å. A third system has been designed, the “hybrid” (H) sample, which uses a cubic silver microcrystal, with a half-spherical cavity on the top, as a substrate for the organic molecule blend (2 PS 16-mers and 52 TMB molecules). The thickness of the organic sample is 25 Å and the total size of the system is approximately $50 \times 50 \times 35$ Å³. The effect of the organic sample boundaries on the confinement of the cascade energy will be addressed in the discussion. For the bombardment itself, a representative set of trajectories are calculated with 500 eV primary Ar atoms uniformly distributed in the impact area and directed along the surface normal. Each trajectory is initiated using a fresh undamaged sample. Open boundary conditions are used for the system. At the end of each trajectory, atoms that have a velocity vector directed away from the surface and are at a height of 8 Å above the top of the sample are considered as sputtered atoms. For identifying clusters, pairs of atoms are checked to see if there is an attractive interaction between them, in which case they are considered linked [12,13]. In all the considered systems, the mass of

hydrogen is taken to be that of tritium (3 amu) to increase computational efficiency [7]. At the end of the trajectories, experimentally observable properties, such as total yield, mass spectrum, kinetic energy and angular distributions are calculated from the final positions, velocities and masses of all the ejected species. Mechanistic information is obtained by monitoring the time evolution of relevant collisional events.

3. Results and discussion

The goal of this study is to understand the different sputtering processes at play when a large organic molecule (PS 16-mer, ~2 kDa) is either adsorbed on a heavy metal substrate or embedded in an organic matrix constituted of smaller molecules. As an introductory example, we describe two representative trajectories corresponding to these cases and where the ejection of the entire PS molecule is observed (Section 3.1). The different mechanisms of the collision cascade development and the molecular motion are investigated via the analysis of specific collision trees [14] and of the position-dependent vertical velocities of the atoms in the sample after the extinction of the collision cascade (Section 3.2). Finally, we comment on the observed decomposition of metastable matrix:analyte clusters (Section 3.3) and on the study of a smaller matrix:analyte sample embedded in a nanoindented inorganic crystal (Section 3.4).

3.1. Examples of trajectories

The time evolution of two typical trajectories, both leading to the ejection of the entire PS molecule, are displayed in Figs. 1 and 2 for samples M and S, respectively. The last frame of each figure shows the fingerprint of the atomic collision cascade induced by the projectile in the target over the first 100 fs of the interaction (collision tree [14]). After a first batch of relatively fast fragments and molecules, the emission in sample M, Fig. 1, proceeds via the swelling and decomposition of the sample surface, frame 2 (3 ps), so that several matrix molecules and the analyte eventually depart in a collective motion, frame 3 (5.5 ps). It should

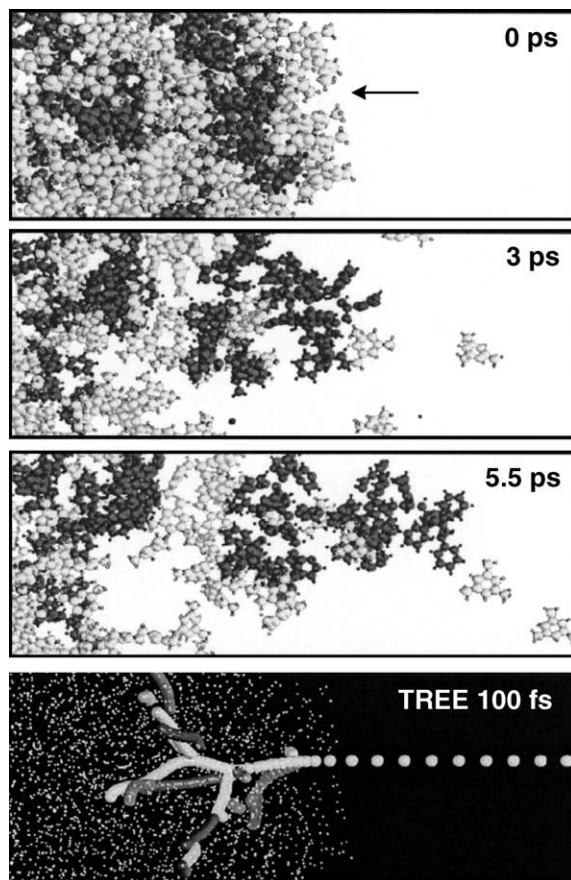


Fig. 1. Frames 1–3: Snapshots of the time evolution of a characteristic trajectory showing the ejection of a large organic cluster, including the entire PS oligomer, from sample M. Light gray spheres correspond to the matrix molecules and dark gray spheres to the PS oligomer. The arrow in frame 1 indicates the projectile trajectory before it reaches the sample surface. Frame 4: Collision tree. Spheres with different shades of gray represent the successive positions of different atoms set in motion with more than 10 eV of kinetic energy in the first 100 fs of the projectile–surface interaction. White dots are atoms at rest in the sample.

be noticed that for such a molecular solid held together by weak van der Waals bonds, the ejected volume at the end of the trajectory roughly corresponds to the initial volume of the collision cascade. In the case of sample S, Fig. 2, the collision cascade develops in the heavy silver substrate, where part of the momentum is already redirected towards the surface during the first hundred of femtoseconds, frame 3. Those upward moving

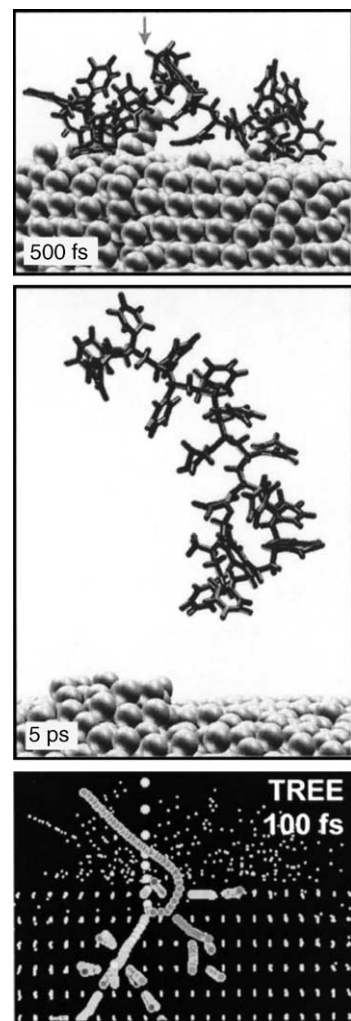


Fig. 2. Frames 1–2: Snapshots of the time evolution of a characteristic trajectory showing the desorption of the entire PS16 oligomer from sample S. The silver atoms are depicted by gray spheres. To emphasize the motions in the silver substrate, only the bonds of the PS molecule are represented (black sticks). The arrow in frame 1 indicates the projectile trajectory before reaching the sample surface. Frame 3: Collision tree (see Fig. 1 caption).

silver atoms distribute their momentum before reaching the surface, generating a larger population of slow metal atoms moving in a collective manner. Analyte emission starts when this population of silver atoms crosses the surface plane and gently pushes several parts of the molecule, frame 1. Most of these silver atoms remain bound to the

surface and the silver crystal tends to recover its integrity after the molecule is ejected, except for a group of dislocated atoms sitting on top of the rearranged surface, frame 2.

3.2. Emission mechanisms

The collision tree corresponding to sample S (Fig. 2) demonstrates that the silver substrate is able to reflect part of the projectile momentum towards the surface via the collision cascade in the first 100 fs following the impact. The mechanism of energy reflection is different in sample M where the collision cascade is downward-directed and almost no motion occurs at the surface of the sample in the first picosecond of the interaction. To investigate this mechanism, the instantaneous z -velocities of the carbon and silver atoms after 200 fs have been plotted as a function of their z -coordinate, Fig. 3. At this time, the atomic collision cascade is over and the remaining action must be attributed to collective motions, including molecular translation, vibration or rotation. In sample M, frame 1, the z -velocities of C atoms range from -5000 to $+5000$ m/s, with a considerable scattering and very few atoms are set in motion near the surface of the sample ($z = 0$ Å). The average curve (black line) fluctuates in the range -1000 to $+500$ m/s, with a slight trend of increasing velocity with increasing z -coordinate. The interpretation of this behavior, supported by the analysis of the trajectory movies, is that the energy is stored in the vibrational modes of the matrix and analyte molecules. The situation of sample S is different, frame 2. There is less scattering in the data and the average curve shows a marked trend of increasing velocity as a function of z . The velocities of the silver atoms are comprised between -3000 (at the bottom of the crystal) and $+2000$ m/s (top of the crystal). The z -dependent average continues to increase beyond the interface, with a more pronounced slope for the C atoms belonging to the PS molecule. The specific structure in the data corresponding to the silver crystal ($z \leq -10$ Å) deserves an explanation. Except for a number of dislocated atoms, the silver planes are distinct and there is a positive correlation between the z -velocities and the z -coordinates in each plane, as

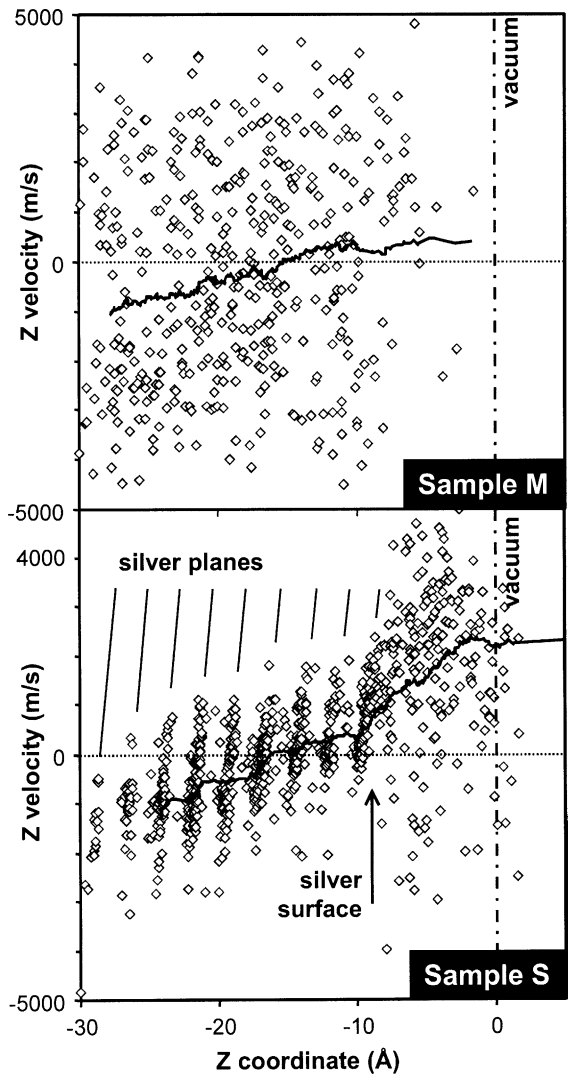


Fig. 3. Instantaneous z -velocities of the C (Ag) atoms plotted as a function of their z -coordinate 200 fs after the beginning of the trajectories for a collection of 50 impact points (1 data point out of 5 is shown for clarity. Positive coordinates and velocities are directed upward. The surface of the sample before bombardment corresponds to $z = 0$. The full lines indicate the z -dependent average velocity (values averaged over 100 data points). Frame 1: sample M and frame 2: sample S.

indicated by the oblique black lines. This correlation means that most of the silver atoms travel away from their initial position in the silver layers (upward motion above the plane and downward motion below the plane). The reason is that, after 200 fs, the energy is being transferred in the

vibrational mode of the crystal. Because the photon periods are close to 1 ps, the atoms are still in the beginning of the first period of vibration, in the process of escaping from their initial lattice positions. Over a longer period of time, the well-defined pattern seen in Fig. 3, frame 2, blurs and disappears gradually, while the energy distributes over the whole sample. When the molecule is ejected at fragments, the C atoms are first pushed downward by the interaction with the projectile and, then, they acquire a relatively large positive velocity and are ejected from the surface because of the action-reaction with the heavy and compact silver substrate. When the molecule is ejected intact, it is because of the concerted push of a group of silver atoms, as shown in Fig. 2. Except for the ejection of a few energetic silver atoms, the strongly bound silver substrate remains a whole until the end of the trajectory. In contrast, the molecular motion in the soft and open medium of sample M is slower and the accumulated vibrational energy eventually induces the decomposition of the loosely bound sample.

3.3. Metastable nanoclusters

The emission of matrix:analyte nanoclusters containing one PS oligomer and a number of matrix molecules is not a rare event in the case of sample M. The statistics of the trajectories show that PS:TMB_x clusters with $1 \leq x \leq 10$ are observed in the simulations. Extended time calculations specifically performed with these clusters demonstrate that all of them decompose in the first 100 ps after emission, because of their high internal energy with respect to the intermolecular van der Waals forces. As an example, Fig. 4 shows two snapshots of the time-evolution of a cluster containing 1 PS oligomer and 7 TMB molecules. After 8.5 ps, the mass of the nanocluster is 3010 Da (considering ${}^3\text{H}$ isotopes instead of H, see Section 2) and its internal energy is 22 eV (see mathematical formula in [8]). Out of influence of the surface, the cluster ejects 5 TMB molecules (9, 18 and 54 ps after projectile impact). Frame 1 displays the situation at 18 ps when the cluster loses a single TMB molecule (number 1) and a TMB dimer (numbers 2–3). After 54 ps, the remaining

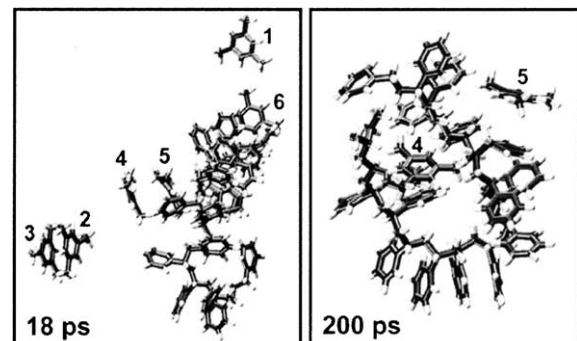


Fig. 4. Snapshots showing the time evolution of a sputtered PS:TMB₇ cluster. Frame 1: 18 ps and frame 2: 200 ps.

PS:TMB₂ cluster remains stable until at least 200 ps, frame 2. The shape of the PS oligomer and the relative positions of the TMB molecules change significantly over that period of time.

3.4. Hybrid sample

To test the influence of the organic sample size and boundary conditions, a sample containing half the organic material of sample M (2 PS and 52 TMB molecules) was embedded in the half-spherical cavity of a larger silver crystal (sample H [15]). Even though the collision cascades mostly develop in the organic medium for sample H, the average number of sputtered atoms is twice as high as for sample M. After the extinction of the collision cascades (~ 200 fs), the vibrationally excited organic medium interacts with the silver crystal that reflects and focuses the momentum upwards. The efficient energy reflection responsible for the yield enhancement can be explained by the weak coupling between the energized organic medium and the inorganic substrate [15]. These results directly evoke the observation that nanoporous silicon substrates enhance molecular species emission in laser ablation experiments (DIOS [16]). They also open new perspectives for SIMS analysis.

4. Conclusion

Classical MD simulations indicate that the emission of a 2 kDa PS molecule can occur either

from a heavy metal substrate or from an organic matrix composed of small molecules (trimethylbenzene). In the “matrix” sample, the interaction between the vibrationally excited volume and the surrounding “cold” medium causes the expansion of the surface matrix and analyte molecules in the vacuum. A major cause of the emission of large amounts of organic material in such a system is the weakness of the intermolecular forces in the organic solid. For the same reason, the desorbed matrix:analyte clusters decompose in the first 100 ps after emission. In the “substrate” sample, part of the projectile momentum is reflected via the collision cascade occurring in the silver crystal, which induces a generation of low energy, upward moving recoil atoms that cross the surface plane and gently push the molecule towards the vacuum. Two important factors explaining the desorption of intact molecules are the collective action of these relatively slow silver atoms and their inefficiency to fragment the PS molecule. Finally, high sputtering yields are also observed when a matrix:analyte sample is embedded in a nanostructured silver crystal. In this latter case, the observed yield enhancement with respect to a purely organic sample is due to the weak energy coupling between the vibrationally excited organic medium and the silver crystal that efficiently induces the reflection of the cumulated momentum towards the sample surface.

Acknowledgements

A.D. acknowledges the Belgian *Fonds National pour la Recherche Scientifique* for financial support. B.A. receives the financial support of the PAI-IUAP P4/10 Belgian Research Program on

“Reduced Dimensionality Systems”. The financial support of the National Science Foundation through the Chemistry Division is gratefully acknowledged by B.J.G. Additional computational resources were provided the Academic Services and Emerging Technologies (ASET) of Penn State University. We are also indebted to the Center for Academic Computing staff for assistance with the Lion-xe cluster.

References

- [1] L.K. Liu, K.L. Busch, R.G. Cooks, Anal. Chem. 53 (1981) 109.
- [2] K.J. Wu, R.W. Odom, Anal. Chem. 68 (1996) 873.
- [3] K. Wittmaak, W. Szymczak, G. Hoheisel, W. Tuszyński, J. Am. Soc. Mass Spectrom. 11 (2000) 553.
- [4] H. Grade, N. Winograd, R.G. Cooks, J. Am. Chem. Soc. 99 (1977) 7725.
- [5] I.V. Bletsos, D.M. Hercules, D. vanLeyen, A. Benninghoven, Macromolecules 20 (1987) 407.
- [6] A. Benninghoven, B. Hagenhoff, E. Niehuis, Anal. Chem. 65 (1993) 630A.
- [7] R. Chatterjee, Z. Postawa, N. Winograd, B.J. Garrison, J. Phys. Chem. B 103 (1999) 151.
- [8] A. Delcorde, X. Vanden Eynde, P. Bertrand, J.C. Vickerman, B.J. Garrison, J. Phys. Chem. B 104 (2000) 2673.
- [9] S.J. Stuart, A.B. Tutein, J.A. Harrison, J. Chem. Phys. 112 (2000) 6472.
- [10] D.W. Brenner, Phys. Rev. B 42 (1990) 9458.
- [11] D.W. Brenner, O.A. Shenderova, J.A. Harrison, S.J. Stuart, B. Ni, S.B. Sinnott, J. Phys.: Condens. Matter 14 (2002) 783.
- [12] D.E. Harrison Jr., C.B. Delaplain, J. Appl. Phys. 47 (1976) 2252.
- [13] A. Wucher, B.J. Garrison, Phys. Rev. B 46 (1992) 4855.
- [14] A. Delcorde, B.J. Garrison, J. Phys. Chem. B 104 (2001) 105, 9474.
- [15] A. Delcorde, B.J. Garrison, J. Phys. Chem. B 107 (2003) 2297.
- [16] J. Wei, J. Buriak, G. Siudzak, Nature 401 (1999) 243.